

# Characteristics of ultraviolet photoluminescence from high quality tin oxide nanowires

Rui Chen, G. Z. Xing, J. Gao, Z. Zhang, T. Wu,<sup>a)</sup> and H. D. Sun<sup>b)</sup>

*Division of Physics and Applied Physics, School of Physical and Mathematical Sciences, Nanyang Technological University, Singapore 637371, Singapore*

(Received 17 June 2009; accepted 24 July 2009; published online 12 August 2009)

We investigate the optical properties of ultraviolet range emission from high quality tin oxide nanowires prepared by vapor-liquid-solid growth technique. Temperature dependent photoluminescence (PL) measurement is performed between 10 and 300 K. At low temperatures, the PL originates from radiative recombination of excitons bound to neutral donors, donor-acceptor pair transition and their associated longitudinal optical (LO) phonon replicas. The LO-phonon replicas up to third order with Huang–Rhys factor of 0.34 are observed. Evolution of the peaks and the origin of PL thermal quenching at high temperatures are discussed in detail. © 2009 American Institute of Physics. [DOI: 10.1063/1.3205122]

Tin oxide ( $\text{SnO}_2$ ) is an important wide band gap material ( $E_g \sim 3.62$  eV at 300 K for bulk), and its alloy with indium, i.e., ITO, has been extensively used as transparent conductor in gas sensor, solar cell, and light emitting diodes.<sup>1,2</sup> It has very large exciton binding energy ( $\sim 130$  meV), even larger than that of ZnO ( $\sim 60$  meV). Such a large exciton binding energy is prerequisite for direct observation of exciton related phenomena even at room temperature.<sup>3</sup> Unfortunately,  $\text{SnO}_2$  is one of the few special materials that the direct band gap is dipole forbidden in the bulk state. Therefore, to pursue the potential for light emitting near the band edge, researchers have paid more attention to explore the luminescence properties of nanostructures, hoping that nanostructured material such as one-dimensional nanowires (NWs) may break the selection rule imposed in their bulk counterparts.<sup>4–11</sup> However, in most of reports, rather than the band edge emission in the ultraviolet (UV) wavelength range,  $\text{SnO}_2$  nanostructures only showed broad emissions in the wavelength range of 400–600 nm at room temperature which is related to deep level defects.<sup>12–16</sup> In order to obtain efficient UV luminescence, superior crystalline quality is imperative.

Very few reports have been published regarding the UV emission of  $\text{SnO}_2$ , especially for nanomaterials.<sup>4,5,10,11</sup> The UV luminescence is believed to originate from the recombination of impurity-related energy levels near the band gap. It is well known that the impurity-related emission should be sensitive to temperature and a temperature dependent photoluminescence (PL) study may help to reveal the detailed emission mechanism. However, in existing publications, the UV emission was either observed at room temperature,<sup>5,10,11</sup> or discussed based on power dependent PL measurement.<sup>4</sup> Up to now, there has been no systematic study of temperature-dependent PL in  $\text{SnO}_2$  materials. In this letter, we report on the strong UV emission at low temperatures related to the near-band-edge transition in  $\text{SnO}_2$  NWs. Temperature evolution of PL measurement was carefully investigated in the range from 10 to 300 K. Spectra pertaining to the exciton bound to neutral donor ( $\text{D}^0\text{X}$ ), donor-acceptor pair (DAP) transition, and their longitudinal optical (LO)

phonon replicas were identified and analyzed.

The sample was fabricated on (111)-oriented silicon wafers using the vapor-liquid-solid technique under optimal growth conditions. Detailed growth mechanism and conditions can be found in Ref. 17. The PL measurements were performed between 10 and 300 K within a closed cycle helium cryostat. A cw He–Cd laser emitting at 325 nm was used as the PL excitation source and the signal was dispersed by a 750 mm monochromator combined with suitable filters, and detected by a photomultiplier using the standard lock-in amplifier technique.

As shown in Fig. 1(a), tangled NWs with a diameter of  $15 \pm 5$  nm were grown on the Si substrate. From the high resolution transmission electron microscope (HRTEM) image of an individual  $\text{SnO}_2$  NW shown in Fig. 1(b), the inter-

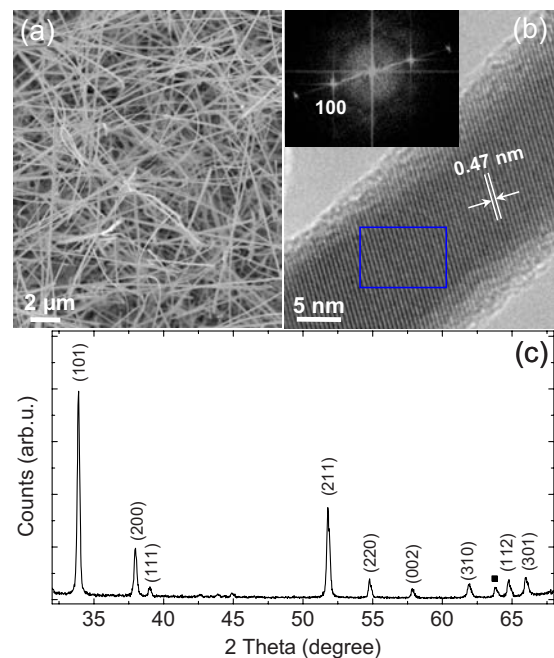


FIG. 1. (Color online) (a) FESEM image of the  $\text{SnO}_2$  NWs. (b) Representative HRTEM image of an individual  $\text{SnO}_2$  NW and the corresponding FFT pattern (inset). (c) XRD pattern of the  $\text{SnO}_2$  NWs grown on the Si substrate. The peak denoted by closed square is due to the Si substrate.

<sup>a)</sup>Electronic mail: tomwu@ntu.edu.sg.

<sup>b)</sup>Electronic mail: hdsun@ntu.edu.sg.

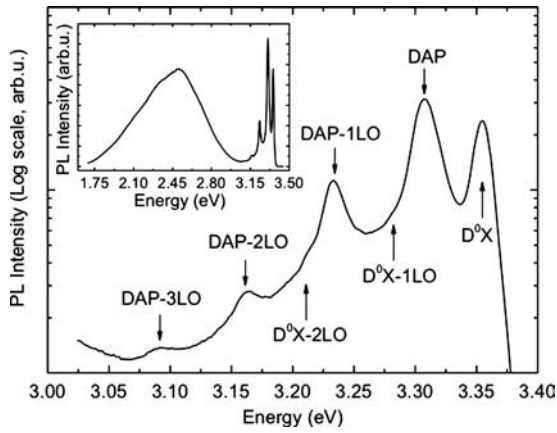


FIG. 2. UV emission of SnO<sub>2</sub> NWs (logarithmic scale) taken at 10 K. The inset shows the whole PL spectrum (linear scale) of the investigated sample.

planar *d*-spacing of 0.47 nm can be indexed as SnO<sub>2</sub> {100} plane which suggests the tetragonal rutile SnO<sub>2</sub> structure and is consistent with the fast Fourier transformation (FFT) pattern results shown in the inset. No structural defect was observed within the detection limit indicating the high crystalline quality of the sample. The x-ray diffraction (XRD) pattern [Fig. 1(c)] also confirms a single crystalline tetragonal rutile SnO<sub>2</sub> structure.

Figure 2 shows the low temperature (10 K) UV range PL spectra of SnO<sub>2</sub> NWs under laser power density around 0.035 W cm<sup>-2</sup>. The inset is the PL spectrum in an extended wavelength range. At low temperatures, the sample exhibits strong UV emission comparable to the broad visible emission band. The visible PL signal may come from the deep level defects such as tin interstitial, dangling bonds, or oxygen vacancies, which will not be discussed here.<sup>17</sup> In Fig. 2, we ascribe the PL peak near 3.307 eV to the transition of DAP in the sample, which is in good agreement with the results reported by other authors regarding single crystalline SnO<sub>2</sub> films.<sup>7</sup> On the high energy side, an emission band peaked at 3.355 eV was observed. Similar feature has been observed in SnO<sub>2</sub> NWs (Ref. 4) and bulk material,<sup>6</sup> but until now, the origin of this peak is not clear yet. We attribute this peak to the radiative recombination of D<sup>0</sup>X, which will be corroborated later. Other emission bands, such as free exciton emission, are absent in the PL spectra of our sample.

It is interesting to note that LO-phonon replicas up to three orders of the DAP band can be easily resolved from the PL spectrum, indicating the high crystalline quality of the sample. In the Franck-Condon model, the electron-LO-phonon coupling strength is described using the Huang-Rhys *S* factor.<sup>18</sup> The relative intensity of the *n*th phonon replicas (*I<sub>n</sub>*) is related to the zero-phonon peak (*I<sub>0</sub>*) by the *S* factor as,

$$I_n = I_0 (S^n e^{-S} / n!), \quad n = 0, 1, 2, \dots \quad (1)$$

From the measured data, the *S* factor associated with DAP is calculated to be approximately 0.34.

The normalized PL spectra (in linear scale) measured in the temperature range between 10 and 300 K are presented in Fig. 3. The intensity of both the PL emission and their LO-phonon replicas decrease exponentially at elevated temperatures. A closer look at the trend of the D<sup>0</sup>X emission band reveals that the relative intensity decreases faster and totally disappears around 70 K, which is the characteristic behavior of exciton bound to neutral donor. As the temperature in-

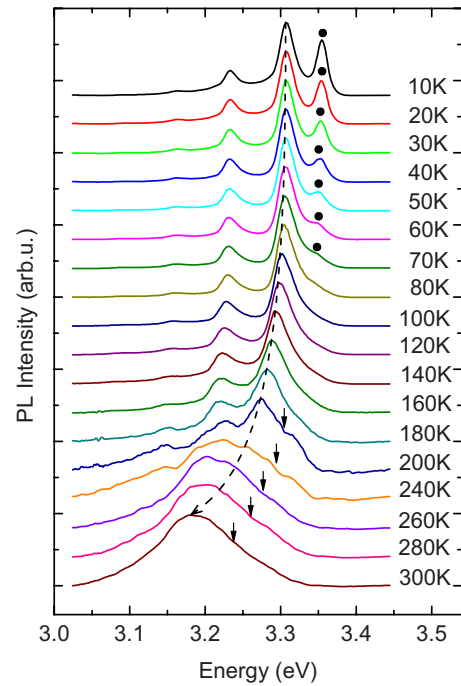


FIG. 3. (Color online) Temperature dependent PL from 10 to 300 K. Dashed line indicates the peak evolution of the DAP peak while the close circles show the trend of D<sup>0</sup>X. The arrows denote the eA<sup>0</sup> transition positions.

creases, it is more probable for the bound excitons to be ionized, and eventually become free excitons. Compared to D<sup>0</sup>X, the DAP transition sustains at higher temperatures, which indicates that the impurities involved have larger binding energies and their ionization requires higher thermal energy. It is well established that at higher temperatures, the DAP transition will transform to the recombination from free electron to acceptor (eA<sup>0</sup>), and this process is associated with an energy slightly higher than that of DAP due to the ionization of electrons bound to neutral donors.<sup>12,19,20</sup> From Fig. 3, it can be seen that at temperatures higher than 200 K, small peaks indicated by arrows emerge at the higher energy side of the DAP transition, which can be ascribed to eA<sup>0</sup>. Despite of the temperature broadening, the difference between DAP and eA<sup>0</sup>, i.e., the donor ionization energy can be estimated to be ~30 meV. When the temperature arises further up to room temperature (300 K), all the PL bands broaden and merge together to form a broad emission band at ~3.18 eV.

Figure 4(a) shows the variation of the PL peak energies of the SnO<sub>2</sub> NWs as a function of temperature. It clearly shows that the energy difference between DAP and its LO-phonon replicas is well defined to be 72.5 meV, slightly smaller than the phonon energy reported in SnO<sub>2</sub> NWs (74 meV).<sup>4</sup> The reason for this discrepancy is not clear, but we speculate that it may result from the phonon zone-folding effect due to the small diameter of the NWs.<sup>21</sup> Such phonon replicas related to the DAP transition have also been observed in the SnO<sub>2</sub> NWs (Ref. 4) and the earlier investigations of ZnO materials.<sup>22,23</sup>

Next, we discuss the temperature dependence of the integrated PL intensity. Since the D<sup>0</sup>X transition disappears around 70 K, we focus on the behavior of DAP in the temperature range from 70 to 300 K. In fact, the temperature dependent integrated PL intensity cannot be fitted with satisfaction using an Arrhenius plot with single thermal activation

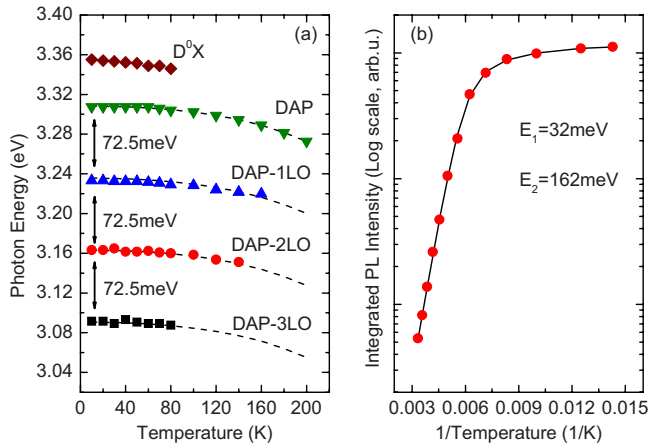


FIG. 4. (Color online) (a) Temperature dependent peak positions of  $D^0X$ , DAP and its 1LO-, 2LO-, and 3LO-phonon replicas. The dashed lines are guide to the eyes. (b) The dependence of the integrated PL intensity on the reciprocal of temperature and the solid curve is the corresponding fit based on Eq. (2).

energy. Instead it can be well described by the following dual activation energy model,<sup>24</sup>

$$I(T) = \frac{I(0)}{[1 + c_1 \exp(-E_1/\kappa T) + c_2 \exp(-E_2/\kappa T)]}, \quad (2)$$

where  $\kappa$  is the Boltzmann constant,  $T$  is temperature,  $E_1$  and  $E_2$  denote the activation energies for two different thermal activation processes, and the parameters  $c_1$  and  $c_2$  are the relative ratios of nonradiative recombination and reflect the competition between the recapture and the nonradiative recombination.

Figure 4(b) shows the integrated PL intensity of the DAP transition in  $\text{SnO}_2$  NWs as a function of temperature from 70 to 300 K. From a least square fitting procedure using Eq. (2), the activation energies obtained are estimated to be 32 and 162 meV, respectively. To make the fitting process meaningful requires a clarification of the physical origin of the two activation processes. The DAP transition is a process by which some of the electrons on the neutral donors combine radiatively with holes on the neutral acceptors. As a result, the neutral donors and the neutral acceptors become ionized donors and ionized acceptors. At high temperatures when the thermal energy is comparable to the donor binding energy, it is easier for electrons to ionize without DAP transition, which results in the decrease of the PL integrated intensity. It is well known that the defect binding energy falls in the range of 5–50 meV for donor and 20–200 meV for acceptor depending on the material parameters.<sup>25</sup> So we can attribute the deduced thermal activation energy of 32 meV to be the donor binding energy and 162 meV to the acceptor binding energy, respectively. We note here that the 32 meV activation

energy is close to the donor ionization energy (30 meV as estimated from Fig. 3), which confirms our previous assignment.

In conclusion, we have investigated the temperature dependent PL in the UV range of very thin  $\text{SnO}_2$  NWs with high crystalline quality. At low temperatures, transition from  $D^0X$ , DAP and their relevant LO-phonon replicas have been observed. LO-phonon replicas up to three orders of the DAP emission with Huang–Rhys factor of 0.34 can be easily resolved from the PL spectrum. The emission mechanisms of impurity related energy levels and their evolution were discussed in detail. Our results indicate that high quality  $\text{SnO}_2$  can serve as an excellent UV emitter, and research down this line may help to advance photonic and sensing devices based on  $\text{SnO}_2$ .

<sup>1</sup>M. Gratzel, *Nature (London)* **414**, 338 (2001).

<sup>2</sup>P. K. H. Ho, J. S. Kim, J. H. Burroughes, H. Becker, S. F. Y. Li, T. M. Brown, F. Cacialli, and R. H. Friend, *Nature (London)* **404**, 481 (2000).

<sup>3</sup>S. Nakamura, *Science* **281**, 956 (1998).

<sup>4</sup>A. Kar, M. A. Stroschio, M. Dutta, J. Kumari, and M. Meyyappan, *Appl. Phys. Lett.* **94**, 101905 (2009).

<sup>5</sup>W. C. Zhou, R. B. Liu, Q. Wan, Q. L. Zhang, A. L. Pan, L. Guo, and B. S. Zou, *J. Phys. Chem. C* **113**, 1719 (2009).

<sup>6</sup>G. Blattner, C. Klingshirn, and R. Helbig, *Solid State Commun.* **33**, 341 (1980).

<sup>7</sup>X. J. Feng, J. Ma, F. Yang, F. Ji, F. J. Zong, C. N. Luan, and H. L. Ma, *Solid State Commun.* **144**, 269 (2007).

<sup>8</sup>J. Jeong, S. P. Choi, C. I. Chang, D. C. Shin, J. S. Park, B. T. Lee, Y. J. Park, and H. J. Song, *Solid State Commun.* **127**, 595 (2003).

<sup>9</sup>S. S. Pan, C. Ye, X. M. Teng, L. Li, and G. H. Li, *Appl. Phys. Lett.* **89**, 251911 (2006).

<sup>10</sup>C. M. Liu, X. T. Zu, Q. M. Wei, and L. M. Wang, *J. Phys. D: Appl. Phys.* **39**, 2494 (2006).

<sup>11</sup>M. Lai, J. H. Lim, S. Mubeen, Y. Rheem, A. Mulchandani, M. A. Deshusses, and N. V. Myung, *Nanotechnology* **20**, 185602 (2009).

<sup>12</sup>J. S. Jie, G. Z. Wang, Y. M. Chen, X. H. Han, Q. T. Wang, B. Xu, and J. G. Hou, *Appl. Phys. Lett.* **86**, 031909 (2005).

<sup>13</sup>X. T. Zhou, F. Heigl, M. W. Murphy, T. K. Sham, T. Regier, I. Coulthard, and R. I. R. Blyth, *Appl. Phys. Lett.* **89**, 213109 (2006).

<sup>14</sup>S. H. Sun, G. W. Meng, G. X. Zhang, J. P. Masse, and L. D. Zhang, *Chem. Eur. J.* **13**, 9087 (2007).

<sup>15</sup>Z. Y. Huang and C. F. Chai, *Mater. Lett.* **61**, 5113 (2007).

<sup>16</sup>S. H. Luo, J. Y. Fan, W. L. Liu, M. Zhang, Z. T. Song, C. L. Lin, X. L. Wu, and P. K. Chu, *Nanotechnology* **17**, 1695 (2006).

<sup>17</sup>Z. Zhang, J. Gao, L. M. Wong, J. G. Tao, L. Liao, Z. Zheng, G. Z. Xing, H. Y. Peng, T. Yu, Z. X. Shen, C. H. A. Huan, S. J. Wang, and T. Wu, *Nanotechnology* **20**, 135605 (2009).

<sup>18</sup>Y. Toyozawa and J. Hermanson, *Phys. Rev. Lett.* **21**, 1637 (1968).

<sup>19</sup>L. J. Wang and N. C. Giles, *Appl. Phys. Lett.* **84**, 3049 (2004).

<sup>20</sup>B. P. Zhang, N. T. Binh, Y. Segawa, K. Wakatsuki, and N. Usami, *Appl. Phys. Lett.* **83**, 1635 (2003).

<sup>21</sup>C. H. Chen, Y. F. Chen, S. An, S. C. Lee, and H. X. Jiang, *Appl. Phys. Lett.* **78**, 3035 (2001).

<sup>22</sup>T. B. Hur, G. S. Jeon, Y. H. Hwang, and H. K. Kim, *J. Appl. Phys.* **94**, 5787 (2003).

<sup>23</sup>K. Thonke, T. Gruber, N. Teofilov, R. Schönfelder, A. Waag, and R. Sauer, *Physica B* **308**, 945 (2001).

<sup>24</sup>H. D. Sun, S. Calvez, M. D. Dawson, J. A. Gupta, G. C. Aers, and G. I. Sproule, *Appl. Phys. Lett.* **89**, 101909 (2006).

<sup>25</sup>C. Klingshirn, *Semiconductor Optics* (Springer, Berlin, 2007).